European Journal of Medical Research

RESEARCH

Open Access

Inhibiting cathepsin B alleviates acute lung injury caused by sepsis through suppression of pyroptosis in lung epithelial cells

Xiaobo Zhang[1], Zhuojun Deng[1*], Xinyu Zhang[1], Qian Xu[1], Li Liu[1], Dong Yang[1] and Zimeng Guo[2]

Abstract

Sepsis-induced lung injury is a serious complication that contributes to the high morbidity and mortality rates in septic patients. This study aims to identify genes associated with sepsis-induced lung injury and evaluate the role of cathepsin B (CTSB) in this process. Here, by analyzing three data sets of sepsis-induced lung injury in mouse models, we identified 23 common differentially expressed genes and performed enrichment analyses. Further experiments demonstrated that CTSB expression was significantly upregulated in the sepsis mouse model, and pre-treatment with the CTSB inhibitor CA-074 markedly improved the survival rate of the mice from 21.05 to 78.95%. In addition, the CTSB inhibitor reduced the systemic inflammatory response in septic mice by decreasing plasma levels of nitric oxide (NO) and the inflammatory cytokines TNF-α and IL-1β.Histological analysis showed that the CTSB inhibitor effectively suppressed CLP-induced lung tissue alterations and neutrophil infiltration, and significantly reduced the expression of inducible nitric oxide synthase (iNOS). Analysis of cell death indicated that the CTSB inhibitor decreased cell death in the lung tissue of CLP mice, particularly by inhibiting the upregulation of gasdermin D-N (GSDMD-N), which is associated with pyroptosis. Furthermore, in vitro experiments revealed that overexpression of CTSB enhanced cell death and promoted pyroptosis in lung epithelial cells. These results indicate that CTSB plays a crucial role in sepsis-induced lung injury, potentially exacerbating the inflammatory response by promoting pyroptosis. Therefore, CTSB may be a potential therapeutic target for sepsis-induced lung injury.

Highlights

- The expression of CTSB significantly increases during sepsis.
- The efficacy of CTSB inhibition in suppressing pyroptosis in lung epithelial cells and alleviating lung injury.
- Overexpression of CTSB can induce pyroptosis in lung epithelial cells.

Keywords Sepsis, Cathepsin B, Inflammation, Pyroptosis, Gasdermin D

*Correspondence:
Zhuojun Deng
37700469@hebmu.edu.cn
[1] Department of Emergency, Hebei Medical University Third Hospital, Shijiazhuang 050000, Hebei, People's Republic of China
[2] Department of Rehabilitation, Hebei Medical University Third Hospital , Shijiazhuang, Hebei, People's Republic of China

Introduction

Sepsis, a life-threatening organ dysfunction caused by a dysregulated host response to infection, affects over 11 million people globally annually with a mortality rate exceeding 20% [1]. Acute lung injury (ALI) and acute respiratory distress syndrome (ARDS) are common and severe complications of sepsis [2]. Characterized by high

incidence and mortality rates, they primarily manifest as pulmonary neutrophil infiltration [3], pulmonary edema [4], and significant cytokine storm, leading to extensive lung damage [5]. The cytokine storm, marked by excessive release of pro-inflammatory mediators, such as interleukin-6 (IL-6), tumor necrosis factor-alpha (TNF-α), and interleukin-1 beta (IL-1β), drives systemic inflammation and multi-organ dysfunction in sepsis. Recent advances in inflammatory process quantification, including enzyme-linked immunosorbent assays (ELISA), multiplex cytokine profiling, and histopathological scoring, have enabled precise evaluation of sepsis severity and therapeutic outcomes. For instance, elevated serum levels of IL-6 and TNF-α correlate strongly with disease progression and mortality in clinical and experimental sepsis, highlighting their utility as biomarkers [6]. These quantitative approaches are critical for dissecting the mechanisms of sepsis-induced ALI/ARDS and identifying novel therapeutic targets.

ALI/ARDS affect an estimated 3 million patients globally each year, with sepsis accounting for 60–70% of cases and contributing to prolonged mechanical ventilation, intensive care unit (ICU) stay, and long-term respiratory dysfunction [7, 8]. Pyroptosis, a recently characterized form of inflammatory cell death, involves the activation of inflammasomes [9], the formation of membrane pores, and the release of pro-inflammatory cytokines [10]. Unlike apoptosis—a programmed cell death pathway devoid of inflammatory responses—pyroptosis not only results in cell demise but also amplifies inflammatory damage [11]. Activation of the NOD-like receptor family pyrin domain-containing 3 (NLRP3) inflammasome facilitates the conversion of pro-caspase-1 into its active form, caspase-1, which subsequently cleaves gasdermin D (GSDMD) to induce pyroptosis [11]. GSDMD-mediated epithelial cell pyroptosis is implicated in the pathogenesis of various pulmonary diseases, including asthma, fibrosis, pneumonia, and ALI/ARDS [12]. Numerous studies have demonstrated that attenuating NF-κB/NLRP3-mediated epithelial cell pyroptosis can ameliorate lipopolysaccharide (LPS)-induced lung injury, underscoring the significance of targeting pyroptosis inhibition in the progression of ALI/ARDS [13].

Gasdermin D (GSDMD) is a crucial protein involved in pyroptosis, a form of programmed cell death that plays a pivotal role in the body's immune response to infection and inflammation [14]. Upon cleavage by inflammatory caspases—such as caspase-1 and caspase-11—GSDMD releases its N-terminal fragment, which subsequently forms pores in the plasma membrane of cells. This pore formation leads to cell swelling, lysis, and the release of pro-inflammatory cytokines, such as interleukin-1β (IL-1β) and interleukin-18 (IL-18), thereby amplifying the inflammatory response [15]. In patients with pre-existing lung disorders (e.g., chronic obstructive pulmonary disease, interstitial lung disease), sepsis and septic shock significantly increase the risk of developing ALI/ARDS, with mortality rates escalating to 50–60% compared to 30–40% in patients without baseline lung injury [16]. The uncontrolled activation of pyroptosis mediated by GSDMD contributes to tissue damage, organ dysfunction, and the systemic inflammation characteristic of sepsis [17]. Elucidating the role of GSDMD in sepsis is paramount, as it not only illuminates the mechanisms underlying this condition but also highlights GSDMD as a potential therapeutic target. Modulating GSDMD activity could unveil new strategies for controlling inflammation and improving outcomes in sepsis and related inflammatory diseases.

CTSB, a cysteine protease of the lysosomal cathepsin family, plays a crucial role in various biological processes, including protein degradation, intracellular signaling, and apoptosis [18]. Predominantly localized within lysosomes, CTSB degrades a broad spectrum of substrates, encompassing extracellular matrix proteins as well as endogenous and exogenous proteins [19]. In the context of pyroptosis, CTSB has been shown to play a significant role [20]. Preclinical studies have demonstrated that CTSB inhibitors reduce NLRP3 inflammasome activation and pyroptosis-related cytokine release in sepsis models, leading to improved survival and attenuated organ injury [21]. Clinically, elevated CTSB activity correlates with disease severity in sepsis patients, particularly those with lung injury, providing a rationale for targeting CTSB to disrupt the pyroptosis-driven inflammatory cascade [22]. It modulates inflammatory responses by activating pro-inflammatory cytokines, thereby promoting the pyroptotic process through the activation of inflammasomes [23]. In sepsis—a severe systemic response to infection—CTSB levels and activity are often elevated, contributing to the enhanced release of pro-inflammatory cytokines and the exacerbation of tissue damage [24]. This involvement of CTSB in both pyroptosis and sepsis underscores its potential as a biomarker and therapeutic target for inflammatory diseases, making it a critical focus of ongoing research aimed at understanding and treating these conditions.

This study aims to elucidate the role and mechanisms of CTSB in the pathophysiology of sepsis-induced ALI and ARDS. First, we evaluated the expression of CTSB in the gene expression omnibus (GEO) data sets of sepsis-induced lung injury in mice, as well as in the gene expression profiles of the cecal ligation and puncture (CLP)-induced lung injury mouse model. Second, using CTSB inhibitors, we investigated the specific role of

CTSB in mediating CLP-induced cell pyroptosis and lung injury.

Materials and methods

Microarray data collection

Microarray data sets GSE40180, GSE23767, and GSE60088 were retrieved from the Gene Expression Omnibus (GEO) database (http://www.ncbi.nlm.nih.gov/geo/). These data sets were used to analyze differential gene expression in lung injury caused by sepsis. The search terms used were "sepsis" and "lung."

Gene ontology (GO) and KEGG pathway enrichment analysis

GO enrichment and KEGG pathway analyses were performed using R software (version 4.2.1, R Foundation for Statistical Computing, Austria). A significance threshold of $p < 0.05$ was applied. GO analysis encompassed three categories: cellular component (CC), biological process (BP), and molecular function (MF). The top 30 enriched pathways were selected to build the KEGG pathway network for visualization.

Animals and experimental design

C57BL/6 mice *(6–8-week-old male, Sibeifu Company, China, animal certificate number: SCXK (Jing) 2021–0004)* were maintained in a pathogen-free environment at controlled conditions of 22 ± 2 °C with a 12-h light/dark cycle. They had free access to food. All animal experiments were conducted in strict accordance with the guidelines of the Ethics Committee of Hebei Medical University. To induce sepsis, mice underwent cecal ligation and puncture (CLP). Mice were euthanized 12-day post-surgery. After the study, the lungs were washed with PBS. The left lower lobe of the lung was preserved in 4% formalin for histopathological evaluation, while the remaining lobes were stored at − 80 °C for Western blotting and quantitative PCR (qPCR) analysis.

The project has been approved by the Animal Welfare and Ethics Committee of Hebei Medical University, with approval number IACUC-Z2023-009-1. In this study, 3–4% isoflurane concentration was used for induction of anesthesia. Euthanasia was performed by overdose inhalation of isoflurane, following the ARRIVE guidelines.

The CLP procedure was performed to induce polymicrobial sepsis in mice, as previously described with modifications. In brief, mice were anesthetized via isoflurane inhalation (induction: 4% isoflurane in 100% oxygen at 1 l/min; maintenance: 2% isoflurane in 100% oxygen). Anesthesia depth was assessed by the absence of a pedal reflex. The abdominal area was shaved and disinfected with 70% ethanol. A midline laparotomy (approximately 1 cm) was performed to expose the cecum, which was then exteriorized. A 4–0 silk suture was used to ligate the cecum at approximately 75% of its length, ensuring the maintenance of intestinal continuity. The ligated cecum was punctured twice with a 21-gauge needle to induce fecal leakage into the peritoneal cavity. A small amount of fecal material was extruded through the puncture sites to confirm consistent sepsis induction. The cecum was returned to the abdominal cavity, and the laparotomy incision was closed in two layers: 4–0 absorbable sutures for the muscle layer and surgical staples for the skin. Sham-operated mice underwent the same procedure, including cecum exteriorization, but without ligation or puncture. Postoperatively, mice were resuscitated with 1 ml of pre-warmed sterile saline administered subcutaneously to prevent dehydration, and were placed on a heating pad until fully recovered from anesthesia.

Survival analysis using Kaplan–Meier curves

To evaluate the impact of CTSB on sepsis mortality, a 12-day survival study was conducted using the cecal ligation and puncture (CLP) model. *Sample size was determined using power analysis (G*Power 3.1 software) with an estimated effect size (Cohen's d) of 0.8, $\alpha = 0.05$, and 80% statistical power, resulting in 19 mice per group to detect significant differences.* Mice were randomly assigned to one of four groups: (1) sham-operated controls ($n = 19$), (2) CLP-induced sepsis ($n = 19$), (3) *Sham-operated controls pre-treated with the CTSB inhibitor CA-074 (Sigma-Aldrich, USA, Cat#134448-10-5) (0.05 ml/kg, intraperitoneal injection, 1 h prior to surgery),* and (4) CLP-induced sepsis with pre-treatment of CA-074 (0.05 ml/kg, $n = 19$). Mortality was monitored daily for 12 days. Kaplan–Meier survival curves were generated to compare survival probabilities across groups. Statistical significance was evaluated using the log-rank test, with a $p < 0.05$ considered significant. Hazard ratios (HR) and 95% confidence intervals (CI) were calculated to quantify the effect of CTSB inhibition on survival.

Cell culture

A549 cells (Procell, China, Cat#CL0016) were cultured in *RPMI 1640 medium (Gibco, USA, Cat# 11875093)* supplemented with 10% *fetal bovine serum (FBS, Gibco, USA, Cat# 10099141)* and 100 U/ml *penicillin–streptomycin (Solarbio, China, Cat# P1400).*

Immunohistochemistry and immunofluorescence of lung samples

In brief, 4 μm thick sections were deparaffinized and rehydrated, then transferred to citrate buffer (pH = 6.0) for antigen retrieval and cooled for 20 min. Following incubation with normal goat serum *(Servicebio, China, Cat#SL038)*, the lung sections were incubated with a

primary antibody against iNOS *(Proteintech, China, Cat# 189851-AP)*. Detection was performed using immunofluorescence co-staining with CTSB *(Abcam, UK, Cat# ab125067)* according to standard protocols. Stained sections were imaged using a fluorescence microscope (Olympus, Japan).

Lung wet-to-dry (W/D) weight ratio

The W/D weight ratio was used to evaluate pulmonary edema. Freshly excised lung tissue was weighed to determine wet weight. The tissue was then dried at 60 °C for 48 h to determine dry weight. The W/D weight ratio was calculated by dividing the wet weight by the dry weight.

Histological analysis

Lung samples were preserved in 4% formalin before being embedded in paraffin. Sects. "Discussion" μm thick were obtained and stained with hematoxylin and eosin (H&E) according to standard procedures. The extent of lung injury was assessed by two independent, blinded pathologists. This evaluation was based on five predetermined pathological criteria outlined previously. The assessment included the degree of lung inflammation and thickening of the alveolar walls, with scores as follows:

0: Normal tissue, no airway thickening or edema.

1: Minimal cellular infiltration and edema present.

2: Mild-to-moderate inflammatory changes and airway thickening.

3: Moderate cellular infiltration.

4: Moderate-to-significant inflammatory changes.

5: Severe inflammatory damage.

Western blot analysis

Lung tissue and endothelial cell lysates were prepared using cold *RIPA buffer (Beyotime, China, Cat# P0013B)* supplemented with *protease inhibitors (Sigma-Aldrich, USA, Cat# P8340)*. Protein samples (40 μg) were resolved by SDS–PAGE and transferred to *PVDF membranes (Millipore, USA, Cat# IPVH00010)*. After blocking with 5% non-fat dry milk *(BD, USA, Cat# 232100)*, membranes were incubated overnight at 4 °C with the following primary antibodies: anti-LC3 *(Cell Signaling Technology, USA, Cat# 12741)*, anti-C-CASP3 p20 *(Cell Signaling Technology, USA, Cat# 9662)*, anti-P-MLKL *(Cell Signaling Technology, USA, Cat# 74921)*, anti-P62 *(Proteintech, China, Cat# 18420-1-AP)*, anti-CTSB *(Abcam, UK, Cat# ab125067)*, anti-GPX4 *(Proteintech, China, Cat# 14432-1-AP)*, and anti-GSDMD *(Abcam, UK, Cat# ab209845)*. Following primary antibody incubation, membranes were incubated with HRP-conjugated secondary antibodies *(Goat anti-rabbit IgG, Proteintech, China, Cat# SA00001-2; Goat anti-mouse IgG, Proteintech, China, Cat# SA00001-1)* at 25 °C for 1 h. Protein bands were visualized using an enhanced chemiluminescence (ECL) detection system *(Thermo Fisher Scientific, USA, Cat# 34580)*. Band intensity was normalized to GAPDH *(Proteintech, China, Cat# 60004-1-Ig)* and expressed as a relative ratio to the control.

Reverse transcription quantitative polymerase chain reaction (RT-qPCR)

Total RNA was isolated from mouse lung tissue using TRIzol reagent *(Proteintech, USA, Cat# 15596026)*. The RNA was then reverse transcribed *using the PrimeScrip™ RT Reagent Kit (Takara, Japan, Cat# RR037 A)*. Quantitative PCR was performed using SYBR® Premix Ex TaqTM (2x) *(Takara, Japan, Cat# RR820 A)*, and results were detected using the StepOne Plus system (Applied Biosystem, USA). Mouse GAPDH was used as an internal control. Primers were designed using Primer3 software (version 0.4.0) based on mRNA sequences from the NCBI database (CTSB: NM_013471.3; GAPDH: NM_008084.3) and synthesized by Sangon Biotech (China). The primers used were as follows: CTSB: F: CGCGGCTCAAAA GGAAACC; R: TTAACTTGACAG GGTGAAGCTG. GAPDH: F: TGTTGCCATCAATGACCCCTT; R: CTC CACG ACGTACTCAGCG.

Overexpression of CTSB gene

The pcDNA–CTSB plasmid *(Thermo Fisher Scientific, USA, Cat# V79020)* was used for overexpression of CTSB, with the empty pcDNA vector as a control. Transfection was carried out using the Lipofectamine RNAiMAX transfection reagent *(Thermo Fisher Scientific, USA, Cat# 13778030)*.

TUNEL assay

Apoptotic endothelial cells in lung tissue were identified using the TdT-mediated dUTP nick-end labeling staining method with the TUNEL Apoptosis Assay Kit *(Beyotime, China, Cat# C1088)*. Four-micrometer thick lung sections were deparaffinized, hydrated, and treated with proteinase K (20 μg/ml) for 30 min at 37 °C. TUNEL assays were performed according to the manufacturer's instructions. Images captured using ImageJ software were used to quantify positive staining areas. In addition, the assessment of apoptosis was extended to DNA fragments in MLVECs using TUNEL staining according to standard protocols. Endothelial cells were fixed in 4% paraformaldehyde, permeabilized, and washed with PBS. They were then incubated with the TUNEL reaction mixture in a humid dark chamber at 37 °C for 1 h. Nuclear visualization was performed using 4′,6-diamidino-2-phenylindole *(DAPI, Beyotime, Cat# C1002)* as a counterstain, and images were captured using a fluorescence microscope (Olympus, Japan).

Enzyme-linked immunosorbent assay (ELISA)

The concentrations of IL-1β *(Elabscience, China, Cat# E-EL-M0064)*, TNF-α*(Elabscience, China, Cat# E-EL-M0019c)*, and nitric oxide *(NO, Elabscience, China, Cat# E-BC-K035-M)* in lung tissue and cell supernatants were quantified using ELISA kits according to the manufacturer's instructions. For IL-1β and TNF-α measurement, lung tissue samples were homogenized in phosphate-buffered saline (PBS) and centrifuged at 3000 rpm for 10 min at 4 °C to collect the supernatants. Cell supernatants were collected from cultured cells after appropriate treatment and centrifuged to remove debris. The ELISA procedure involved adding the samples to pre-coated plates and incubating them at room temperature for the recommended time. After washing, detection antibodies were added, followed by a substrate solution. The optical density was measured at 450 nm using a microplate reader, and concentrations were calculated based on standard curves. For nitric oxide (NO) assessment, a Griess reagent system was utilized. Briefly, equal volumes of the cell supernatants were mixed with Griess reagents, and the absorbance was measured at 540 nm. NO concentrations were determined using a standard curve generated from known concentrations of sodium nitrite.

Statistical analysis

Data are presented as mean ± standard error of the mean (SEM). Normality was assessed using the Shapiro–Wilk test. Differences between groups were analyzed using one-way ANOVA followed by Tukey's post hoc test in SPSS Statistics 22.0 (IBM, USA). A $p < 0.05$ was considered statistically significant.

Results

Identification of genes associated with sepsis-induced lung injury

To identify genes associated with lung injury, we analyzed three mouse data sets of sepsis-induced lung injury: GSE40180 [25], GSE23767 [26], and GSE60088 [27] (Fig. 1A). The intersection of differentially expressed genes across these data sets was obtained, and the Venn diagram (Fig. 1B) revealed that 23 genes were commonly differentially expressed in all three data sets. We subsequently performed enrichment analyses on these 23 genes. KEGG pathway analysis showed that these genes were predominantly enriched in pathways, such as the NOD-like receptor signaling pathway, lipid metabolism, and atherosclerosis (Fig. 1C). In addition, gene ontology (GO) enrichment analysis indicated that these genes were primarily involved in biological processes related to

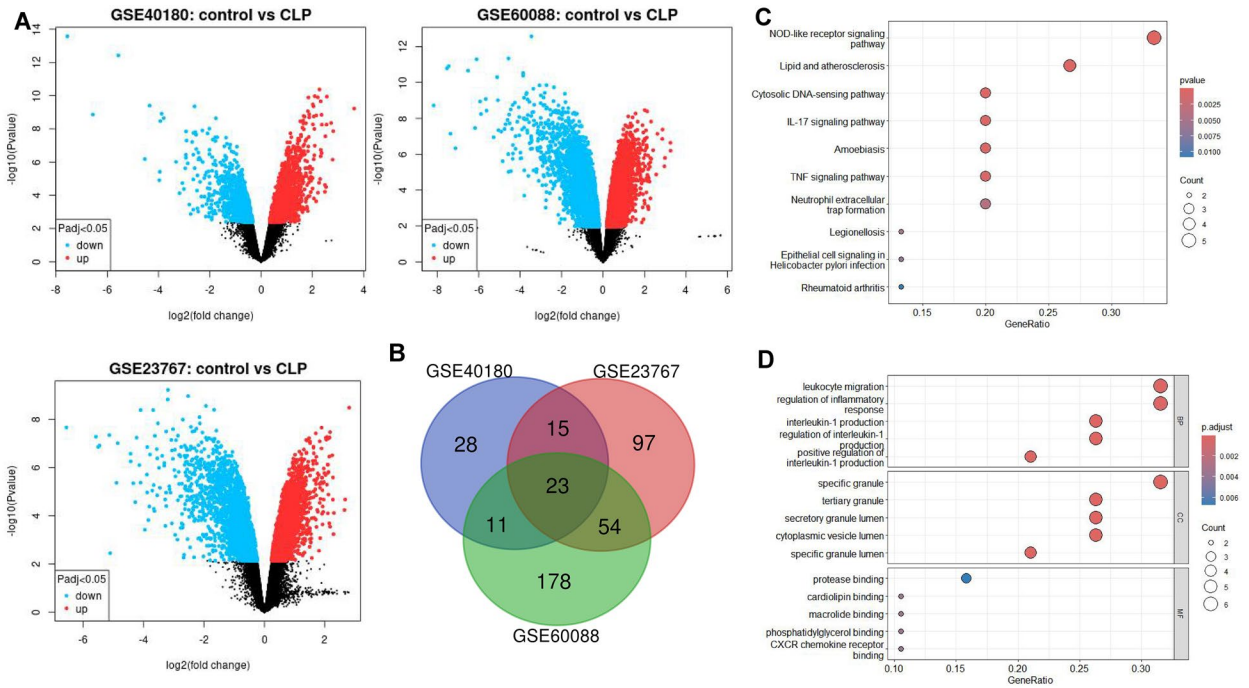

Fig. 1 Identification of genes associated with sepsis-induced lung injury. **A** Volcano plot of differential analysis for GSE40180, GSE23767, and GSE60088. **B** Volcano plot of the intersection genes from GSE40180, GSE23767, and GSE60088. **C** KEGG enrichment analysis. **D** KEGG enrichment analysis

leukocyte migration and the regulation of inflammatory responses (Fig. 1D).

Increased expression of CTSB in lung tissue induced by CLP

We conducted a protein–protein interaction (PPI) analysis on the commonly differentially expressed genes identified from data sets GSE40180, GSE23767, and GSE60088. The findings revealed that CTSB assumes a pivotal role, interacting with the majority of the other genes (Fig. 2A). Upon examining the expression levels of CTSB across these data sets, we observed that CTSB was consistently upregulated in response to sepsis (Fig. 2B). To ensure the accuracy of qPCR results, primer efficiency and stability were validated prior to experimentation. Melting curve analysis demonstrated single sharp peaks for both amplicons, confirming no primer dimers or nonspecific products (Figure S1).Utilizing a murine model to investigate inflammation, Western blot analysis confirmed that CTSB was markedly upregulated in the cecal ligation and puncture (CLP) model (Fig. 2C), with a substantial elevation in CTSB mRNA expression (Fig. 2D). In addition, immunofluorescence analysis demonstrated heightened levels of CTSB protein in the lung tissue of CLP mice (Fig. 2E). Collectively, these data underscore a significant upregulation of CTSB expression following LPS-induced lung injury.

CTSB inhibitor pre-treatment reduces mortality and systemic inflammation in sepsis mice

To investigate the influence of CTSB on sepsis mortality, we monitored the 12-day survival of mice subjected to cecal ligation and puncture (CLP), with or without pre-treatment with the CTSB inhibitor CA-074 (0.05 ml/kg) (Fig. 3A). Kaplan–Meier survival analysis revealed that the 12-day survival rate of mice with CLP-induced sepsis was 21.05%. In contrast, pre-treatment with the CTSB inhibitor significantly improved the survival rate, increasing it to 78.95% (Fig. 3B). All sham-operated control mice survived, irrespective of CTSB inhibitor treatment. Mice subjected to CLP, regardless of CTSB inhibitor pre-treatment, exhibited weight loss during the initial 2 days, followed by subsequent recovery (Fig. 3C). Lung wet-to-dry weight ratios indicated that the CTSB inhibitor did not significantly impact CLP-induced pulmonary edema (Fig. 3D). To assess the effect on nitric oxide (NO) levels, we measured plasma nitrite—an end product of NO—in mice treated with CLP and/or the CTSB inhibitor. Our results demonstrated that serum nitrite levels were markedly elevated in CLP-treated mice, while pre-treatment with the CTSB inhibitor reduced nitrite levels (Fig. 3E).

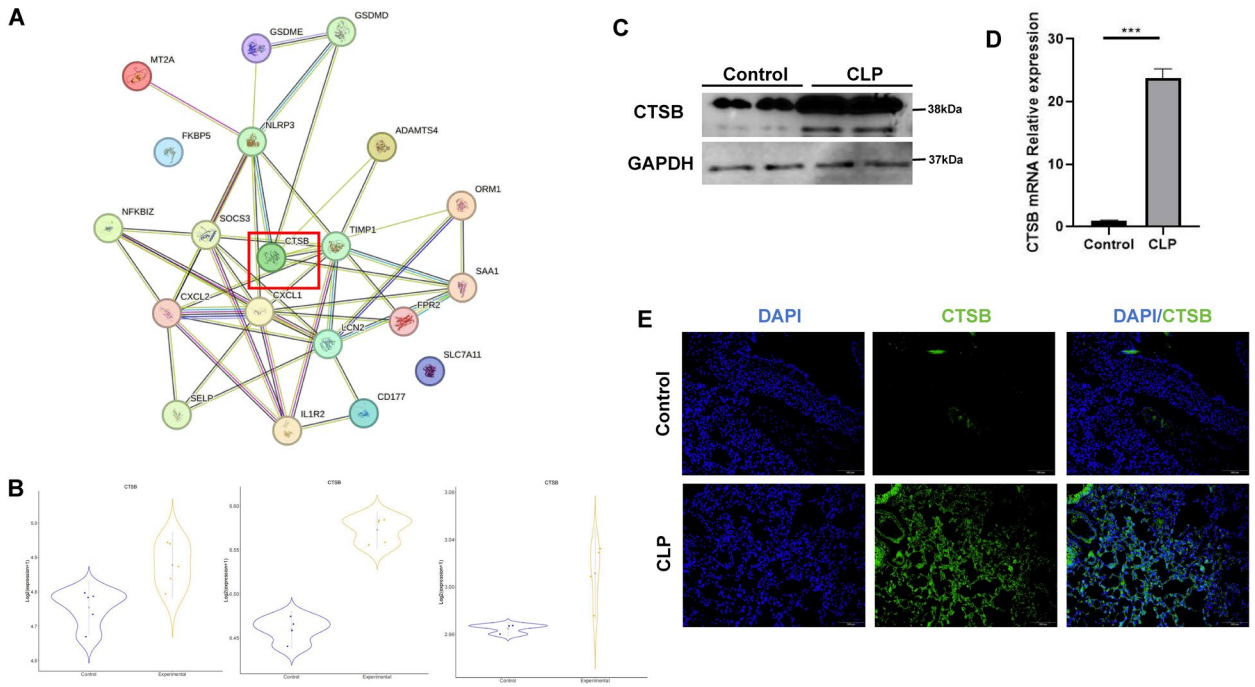

Fig. 2 Increased expression of CTSB in lung tissue induced by CLP. **A** Protein–protein interaction analysis diagram. **B** Expression of CTSB in the data sets GSE40180, GSE23767, and GSE60088. **C** Western blot results demonstrated that CTSB was upregulated in the mouse CLP model. **D** PCR results demonstrated that CTSB was upregulated in the mouse CLP model. **E** Immunofluorescence demonstrated that CTSB was upregulated in the mouse CLP model

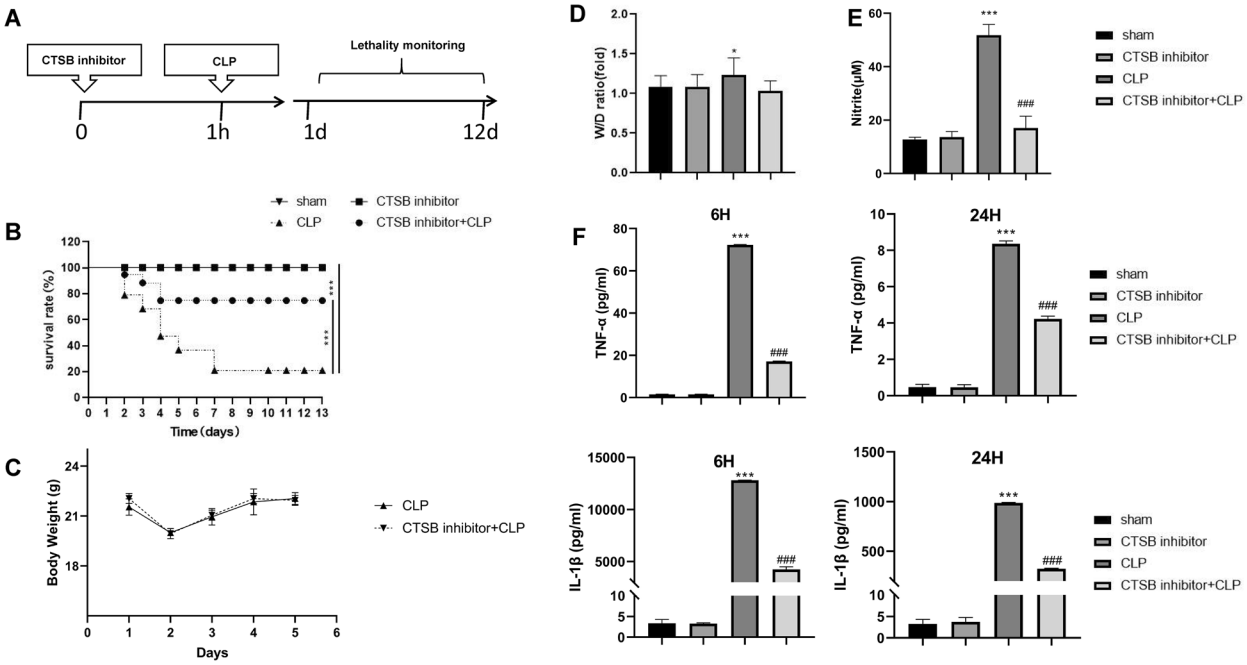

Fig. 3 CTSB inhibitor pre-treatment reduces mortality and systemic inflammation in sepsis mice. **A** Animal experimental model diagram. **B** Mortality curve of the CLP mouse model. **C** Weight change curve of the CLP mouse model. **D** Lung wet–dry weight ratio in the CLP mouse model. **E** Nitrite levels in the CLP mouse model. **F** ELISA measurement of TNF-α and IL-1β levels in mice

Compared to sham-operated control mice, plasma levels of the pro-inflammatory cytokines TNF-α and IL-1β were significantly elevated 6- and 24-h post-CLP. Notably, pre-treatment with the CTSB inhibitor attenuated the CLP-induced increases in both TNF-α and IL-1β levels (Fig. 3F).

CTSB inhibitor pre-treatment suppresses CLP-induced histological changes, neutrophil infiltration, and iNOS gene expression in lung tissue of sepsis mice

Histological alterations in the lungs of septic mice, with or without pre-treatment with a CTSB inhibitor, were evaluated through hematoxylin and eosin (H&E) staining. Lung tissue from control mice injected with saline displayed normal alveolar architecture, devoid of inflammatory cell infiltration. In contrast, the CLP group exhibited pronounced thickening of the alveolar walls, accompanied by extensive infiltration of inflammatory cells (Fig. 4A). To assess neutrophil infiltration, immunofluorescence staining was performed on lung tissues from CLP-induced septic mice, with or without CTSB inhibitor treatment, using an anti-Ly6G antibody to identify neutrophils. The CLP group demonstrated increased immunofluorescence intensity, indicating elevated neutrophil infiltration, whereas pre-treatment with the CTSB inhibitor markedly reduced this infiltration (Fig. 4B, C). Furthermore, we evaluated the expression of inducible nitric oxide synthase (iNOS) in the lung tissues of CLP-treated mice, irrespective of CTSB inhibitor pre-treatment. Immunohistochemical analysis revealed a substantial upregulation of iNOS in the alveolar walls following CLP; however, pre-treatment with the CTSB inhibitor effectively attenuated this upregulation (Fig. 4D, E).

CTSB inhibitor suppresses cell death in vivo

Given the pivotal role of cell death in the inflammatory response during sepsis, we investigated cell death in the lung tissues of CLP-induced septic mice, with or without pre-treatment with a CTSB inhibitor. Our data revealed a significant increase in TUNEL-positive cells in CLP mice, which was markedly reduced following intraperitoneal administration of the CTSB inhibitor (Fig. 5A, B). However, the precise type of cell death occurring in these lung tissues remained unclear. To address this, we analyzed the expression of proteins associated with various forms of cell death, including autophagy (p62 and LC3), apoptosis (CASP3), pyroptosis (GSDMD), necroptosis (MLKL), and ferroptosis (GPX4), using Western blotting. The results demonstrated significant upregulation of cleaved CASP3 and GSDMD-N in the lungs of CLP mice. Notably, the expression of the pyroptosis marker GSDMD-N was significantly downregulated in the lungs of CTSB inhibitor-treated mice (Fig. 5C, D).

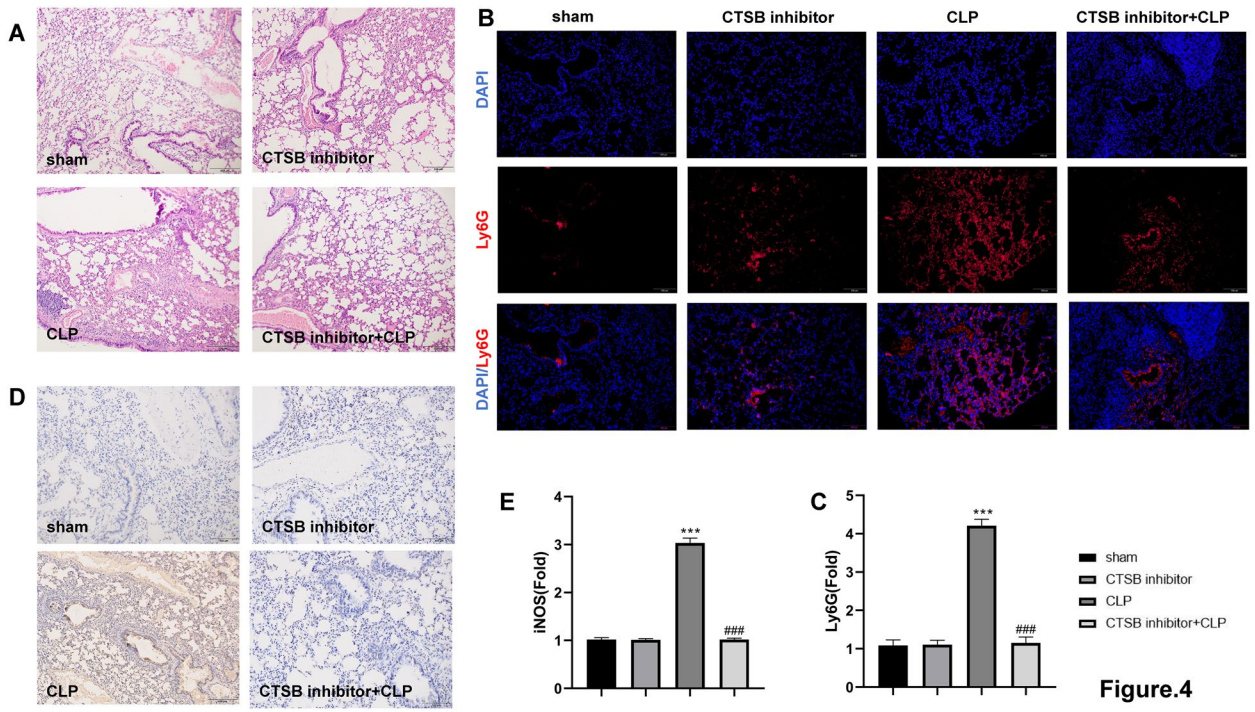

Fig. 4 CTSB inhibitor pre-treatment suppresses CLP-induced histological changes, neutrophil infiltration, and iNOS gene expression in lung tissue of sepsis mice. **A** HE staining of lung tissue from CLP mice. **B**, **C** Immunofluorescence detection of Ly6G expression in lung tissue of the mouse model. **D**, **E** Immunohistochemistry detection of iNOS expression in lung tissue of the mouse model

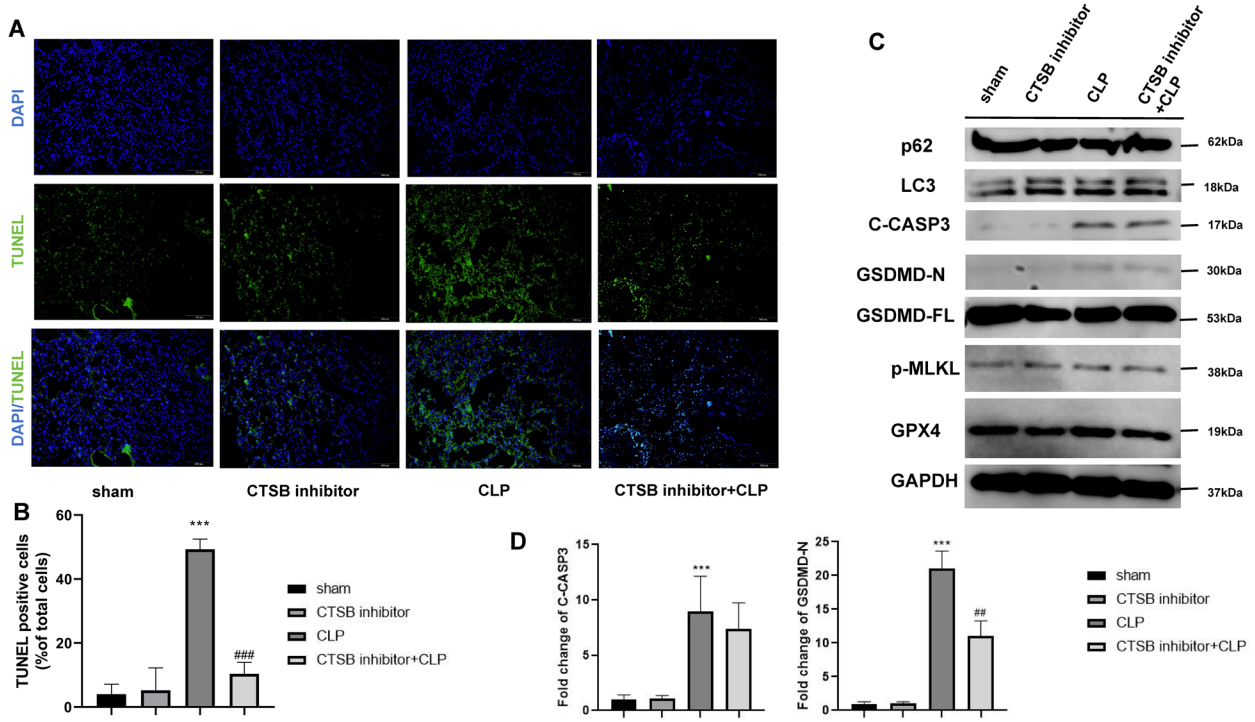

Fig. 5 CTSB inhibitor suppresses cell death in vivo. **A**, **B** Immunofluorescence detection of TUNEL expression in lung tissue of the mouse model. **C**, **D** Western blot analysis of the expression of various death-related proteins in mouse lung tissue

These findings suggest that both apoptosis and pyroptosis occur in the lungs of CLP mice, and that the CTSB inhibitor effectively suppresses CLP-induced pulmonary cell pyroptosis.

CTSB promotes pyroptosis in vitro

To further elucidate the underlying mechanisms, we overexpressed the CTSB gene in the A549 lung epithelial cell line. Our data demonstrated that the OE-CTSB#2 plasmid effectively enhanced CTSB protein expression (Fig. 6A). Following transfection with the CTSB overexpression plasmid, we evaluated cell death by flow cytometry (Fig. 6B, C). The results revealed a significant increase in the number of dead cells upon CTSB overexpression. In addition, the expression of the pyroptosis-associated protein GSDMD-N was markedly upregulated following CTSB overexpression (Fig. 6D, E).

Discussion

In this study, we investigated the role of CTSB in sepsis-induced lung injury, identifying it as a critical mediator of inflammation and cell death mechanisms. Our findings align with Fang et al. who demonstrated that CTSB-mediated autophagy–lysosomal pathway in sepsis-induced acute lung injury [19]. Notably, our observation of GSDMD-N upregulation in CTSB-overexpressing cells corroborates a 2023 study by Meng et al. which highlighted GSDMD-N as a key executor of pyroptosis in cancer immunotherapy [21]. These results reveal that CTSB expression is significantly upregulated in the lungs of mice subjected to CLP, a widely employed experimental model of sepsis. The identification of 23 commonly differentially expressed genes across three independent data sets underscores the central involvement of CTSB in the inflammatory response associated with sepsis-induced lung injury. These findings are consistent with prior research indicating that CTSB participates in diverse forms of cell death, including apoptosis, ferroptosis, and necrosis [28]. For instance, Zhou et al. demonstrated that the lysosomal release of CTSB and cathepsin L (CTSL) promotes the expression of tBid, active caspase-3, and cytoplasmic cytochrome C, thereby driving apoptosis [29]. In contrast to Wang et al. who focused on CTSB-mediated mitochondrial apoptosis in sepsis-induced acute kidney injury, this study highlights a novel role for CTSB in pyroptosis, as evidenced by the downregulation of GSDMD-N in CTSB inhibitor-treated mice [18]. Furthermore, CTSB inhibitors (e.g., CA074) and cathepsin D (CTSD) inhibitors (e.g., pepstatin A) have been shown to significantly attenuate caspase-3 activation and apoptotic cell death [30]. In our investigation, the downregulation or inhibition of CTSB activity ameliorated the severity

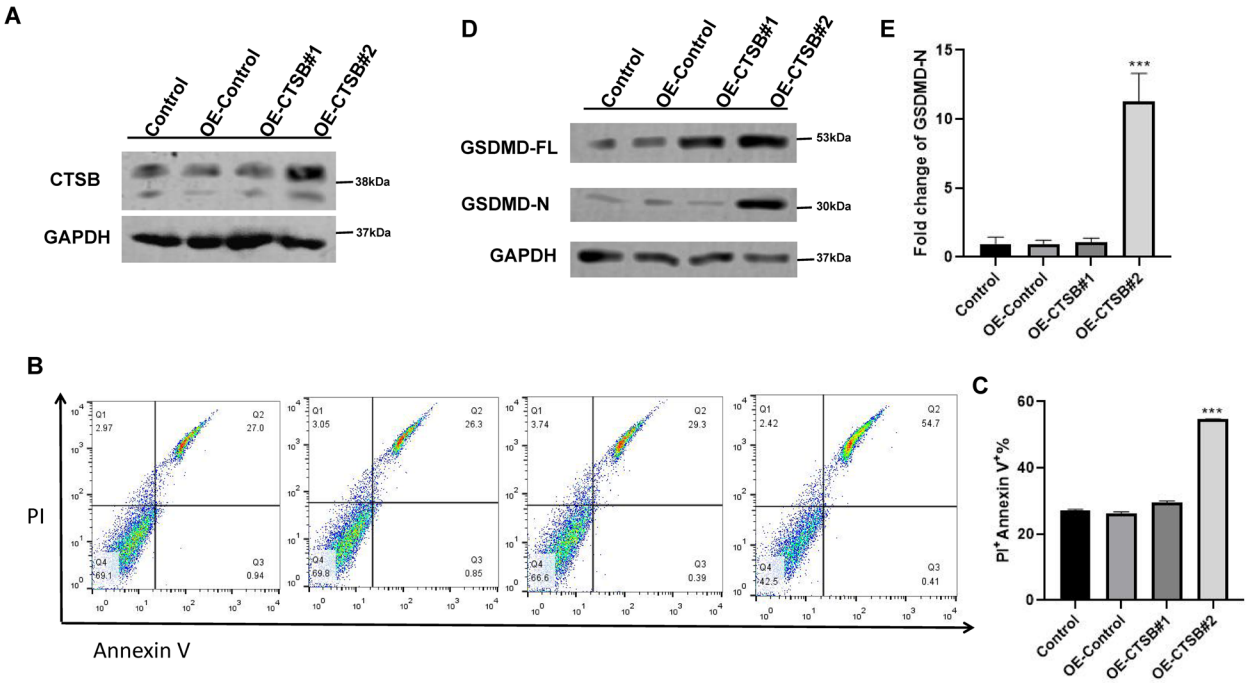

Fig. 6 CTSB promotes pyroptosis in vitro. **A** Detection of CTSB protein expression in A549 cells transfected with overexpressed CTSB. **B**, **C** Flow cytometry analysis of cell death in A549 cells transfected with overexpressed CTSB. **D**, **E** Western blot analysis of GSDMD expression in A549 cells transfected with overexpressed CTSB

of inflammation in sepsis, highlighting the pivotal role of lysosomes and CTSB in the pathophysiology of sepsis-related acute injury. Furthermore, lysosomal membrane permeabilization (LMP) and CTSB may play protective roles in mitigating sepsis-associated acute kidney injury (S-AKI) through modulation of alternative cell death pathways, further emphasizing the multifaceted contribution of CTSB in sepsis. In addition, our findings demonstrate that CTSB substantially induces apoptosis via the mitochondrial pathway in LPS-treated cells, corroborating previous studies [31, 32].

Functional enrichment analysis revealed that the identified genes are involved in key pathways, such as the NOD-like receptor signaling pathway, which plays a pivotal role in the innate immune response [33, 34]. This pathway is known to modulate the activation of inflammasomes, including NLRP3, a key mediator of pyroptosis. Our findings suggest that CTSB may serve as a critical modulator of leukocyte migration and the inflammatory response, both of which are central to the pathophysiology of sepsis and associated pulmonary injury [35]. Administration of a CTSB inhibitor prior to cecal ligation and puncture (CLP) markedly improved survival rates in septic mice, indicating that targeting CTSB may represent a promising therapeutic approach to mitigate sepsis-related mortality. Although the inhibitor did not exert a significant effect on pulmonary edema, it led to a pronounced reduction in systemic inflammation, as evidenced by the diminished levels of plasma nitrite and the pro-inflammatory cytokines TNF-α and IL-1β. These results suggest that CTSB contributes not only to local pulmonary injury but also exacerbates systemic inflammatory responses, thereby complicating the clinical management of sepsis.

Histological analyses showed that treating CLP mice with a CTSB inhibitor markedly reduced neutrophil infiltration and inflammatory cell accumulation in lung tissues. This supports our findings that CTSB promotes cell death, particularly through pyroptosis, as indicated by increased levels of the pyroptosis marker GSDMD-N after CLP [28]. Our in vivo experiments demonstrated that inhibiting CTSB effectively suppressed cell death, highlighting its role in mediating both apoptosis and pyroptosis in sepsis-induced lung injury. In vitro experiments further confirmed that CTSB overexpression in lung epithelial cells promotes pyroptosis. The increased expression of GSDMD-N following CTSB overexpression supports the notion that CTSB is a key regulator of pyroptotic cell death, contributing to the inflammatory cascade observed in sepsis [36].

While this study offers significant insights into the role of cathepsin B (CTSB) in sepsis-induced pulmonary injury, several limitations must be acknowledged. First, our findings are predominantly derived from a murine cecal ligation and puncture (CLP) model, which, though extensively utilized, may not fully replicate the intricate pathophysiology of human sepsis. To enhance the translational relevance of these observations, future studies should aim to validate our results using clinical samples or humanized animal models. Second, while our investigation focused on the contribution of CTSB to pyroptosis and apoptosis, other forms of cell death, such as necroptosis and ferroptosis, may also play a role in sepsis-induced organ damage. Exploring the interactions between CTSB and these alternative cell death pathways could offer a more holistic understanding of sepsis pathogenesis. Third, the CTSB inhibitor employed in this study, CA-074, may possess off-target effects, and its specificity for CTSB in vivo requires further elucidation. Future research should prioritize the development of more selective CTSB inhibitors or genetic approaches, such as CRISPR/Cas9-mediated CTSB knockout, to validate the observed effects. In addition, the timing and dosage of CTSB inhibition may critically influence therapeutic outcomes, and optimizing these parameters could enhance therapeutic efficacy. Finally, while we observed a reduction in systemic inflammation and improved survival with CTSB inhibition, the long-term impact of such treatment on organ function and immune homeostasis remains unclear. Longitudinal studies are necessary to evaluate the potential risks and benefits of targeting CTSB in sepsis. Recent studies, such as those by Chen et al. [37], have expanded our understanding of pyroptosis mechanisms and their interactions with other forms of programmed cell death, such as PANoptosis [38]. These findings underscore the complexity of cell death pathways in sepsis and highlight the need for continued research to identify novel therapeutic targets. Although this study provides valuable insights into the role of CTSB in sepsis-induced lung injury, we recognize the necessity of further investigations to explore additional pyroptosis markers and assess their clinical relevance.

While this study offers significant insights into the role of cathepsin B (CTSB) in sepsis-induced pulmonary injury, several key limitations should be acknowledged to contextualize our findings. First, although we demonstrated CTSB-mediated pyroptosis and apoptosis in a murine CLP model, the translational relevance to human sepsis remains to be confirmed. Murine models may not fully recapitulate human immune responses, such as the differential activation of NLRP3 inflammasome components or cytokine profiles observed in clinical sepsis. Second, while we focused on GSDMD-N as a pyroptosis marker, the specific cell types (e.g., alveolar macrophages vs. epithelial cells) driving CTSB-dependent cell death in lung tissue were not fully delineated. Future studies

using cell-type specific knockout models could clarify this mechanism. Third, the prophylactic administration of CA-074 in this study may not reflect clinical scenarios, where sepsis is often diagnosed after symptom onset. The therapeutic window for CTSB inhibition—particularly when initiated during established sepsis—remains undefined and warrants further investigation. These limitations highlight the need for mechanistic validation in human-derived cells and longitudinal clinical studies to translate our findings into potential therapies.

Conclusion

This study provides compelling evidence that CTSB is a pivotal mediator in sepsis-induced pulmonary injury. Pre-treatment with a CTSB inhibitor markedly enhanced 12-day survival rates from 21.05 to 78.95% ($p < 0.01$), attenuated systemic inflammation, and mitigated cell death, thereby underscoring its therapeutic potential.

Acknowledgements
None.

Author contributions
Xiaobo Zhang conceived and wrote the paper.Xinyu Zhang, Qian Xu, Li Liu, Dong Yang and Zimeng Guo analyzed the materials and drafted the manuscript. Zhuojun Deng revised the whole paper. All authors have reviewed the final version of the manuscript and approved to submit to your journal.

Funding
Hebei Provincial Party Committee Construction Project (20230712).

Availability of data and materials
No datasets were generated or analysed during the current study.

Declarations

Ethics approval and consent to participate
The project has been approved by the Animal Welfare and Ethics Committee of Hebei Medical University, with approval number IACUC-Z2023-009-1. Euthanasia was performed by overdose inhalation of isoflurane, following the ARRIVE guidelines.

Consent for publication
All authors have agreed to publish this manuscript.

Competing interests
The authors declare no competing interests.

Received: 14 April 2025 Accepted: 11 May 2025
Published online: 20 May 2025

References

1. Saito H. Sepsis in Global Health: current global strategies to fight against sepsis. Acute Med Surg. 2025;12: e70045.
2. Mai J, He Q, Liu Y, Hou Y. Hyperoside attenuates sepsis-induced acute lung injury (ALI) through autophagy regulation and inflammation suppression. Mediators Inflamm. 2023;2023:1257615.
3. Qi X, Yu Y, Sun R, Huang J, Liu L, Yang Y, et al. Identification and characterization of neutrophil heterogeneity in sepsis. Crit Care Lond Engl. 2021;25:50.
4. Sánchez Marteles M, Urrutia A. Acute heart failure: acute cardiogenic pulmonary edema and cardiogenic shock. Med Clin. 2014;142(Suppl 1):14–9.
5. Shi Y, Chen W, Du Y, Zhao L, Li Q. Damage effects of bisphenol A against sepsis induced acute lung injury. Gene. 2023;878: 147575.
6. Moldovan F. Role of serum biomarkers in differentiating periprosthetic joint infections from aseptic failures after total hip arthroplasties. J Clin Med. 2024;13:5716.
7. Ortiz G, Garay M, Mendoza D, Cardinal-Fernández P. Impact and safety of open lung biopsy in patients with acute respiratory distress syndrome (ARDS). Med Intensiva. 2019;43:139–46.
8. Lindstedt S, Wang Q, Niroomand A, Stenlo M, Hyllen S, Pierre L, et al. High resolution fluorescence imaging of the alveolar scaffold as a novel tool to assess lung injury. Sci Rep. 2024;14:6662.
9. Jiao Y, Zhang T, Zhang C, Ji H, Tong X, Xia R, et al. Exosomal miR-30d-5p of neutrophils induces M1 macrophage polarization and primes macrophage pyroptosis in sepsis-related acute lung injury. Crit Care Lond Engl. 2021;25:356.
10. Burdette BE, Esparza AN, Zhu H, Wang S. Gasdermin D in pyroptosis. Acta Pharm Sin B. 2021;11:2768–82.
11. Vasudevan SO, Behl B, Rathinam VA. Pyroptosis-induced inflammation and tissue damage. Semin Immunol. 2023;69: 101781.
12. Subramanian S, Geng H, Tan X-D. Cell death of intestinal epithelial cells in intestinal diseases. Sheng Li Xue Bao. 2020;72:308–24.
13. Guo Y, Zhang H, Lv Z, Du Y, Li D, Fang H, et al. Up-regulated CD38 by daphnetin alleviates lipopolysaccharide-induced lung injury via inhibiting MAPK/NF-κB/NLRP3 pathway. Cell Commun Signal CCS. 2023;21:66.
14. Wang K, Sun Q, Zhong X, Zeng M, Zeng H, Shi X, et al. Structural mechanism for GSDMD targeting by autoprocessed caspases in pyroptosis. Cell. 2020;180:941-955.e20.
15. Shi J, Zhao Y, Wang K, Shi X, Wang Y, Huang H, et al. Cleavage of GSDMD by inflammatory caspases determines pyroptotic cell death. Nature. 2015;526:660–5.
16. Qiao X, Yin J, Zheng Z, Li L, Feng X. Endothelial cell dynamics in sepsis-induced acute lung injury and acute respiratory distress syndrome: pathogenesis and therapeutic implications. Cell Commun Signal CCS. 2024;22:241.
17. Shao R, Lou X, Xue J, Ning D, Chen G, Jiang L. Review: the role of GSDMD in sepsis. Inflamm Res Off J Eur Histamine Res Soc Al. 2022;71:1191–202.
18. Wang Y, Xi W, Zhang X, Bi X, Liu B, Zheng X, et al. CTSB promotes sepsis-induced acute kidney injury through activating mitochondrial apoptosis pathway. Front Immunol. 2022;13:1053754.
19. Fang Q, Jing G, Zhang Y, Wang H, Luo H, Xia Y, et al. Erbin accelerates TFEB-mediated lysosome biogenesis and autophagy and alleviates sepsis-induced inflammatory responses and organ injuries. J Transl Med. 2023;21:916.
20. Liu Y, Feng L, Hou G, Yao L. Curcumin elevates microRNA-183-5p via Cathepsin B-mediated phosphatidylinositol 3-Kinase/AKT pathway to strengthen lipopolysaccharide-stimulated immune function of sepsis mice. Contrast Media Mol Imaging. 2022;2022:6217234.
21. Meng Z, Gao M, Wang C, Guan S, Zhang D, Lu J. Apigenin alleviated high-fat-diet-induced hepatic pyroptosis by mitophagy-ROS-CTSB-NLRP3 pathway in mice and AML12 cells. J Agric Food Chem. 2023;71:7032–45.
22. Lu J, Chen Z, Bu X, Chen S, Guan S. Elaidic acid induced hepatocyte pyroptosis via autophagy-CTSB-NLRP3 pathway. Food Chem Toxicol Int J Publ Br Ind Biol Res Assoc. 2023;181: 114060.
23. Zhou H, Du R, Li G, Bai Z, Ma J, Mao C, et al. Cannabinoid receptor 2 promotes the intracellular degradation of HMGB1 via the autophagy-lysosome pathway in macrophage. Int Immunopharmacol. 2020;78: 106007.
24. Almansa R, Herrero-Rodríguez C, Martínez-Huélamo M, Vicente-Andres MDP, Nieto-Barbero JA, Martín-Ballesteros M, et al. A host transcriptomic signature for identification of respiratory viral infections in the community. Eur J Clin Invest. 2021;51: e13626.
25. Ektesabi AM, Mori K, Tsoporis JN, Vaswani CM, Gupta S, Walsh C, et al. Mesenchymal stem/stromal cells increase cardiac miR-187-3p expression in a polymicrobial animal model of sepsis. Shock. 2021;56:133–41.
26. Zhou S, Zhao W, Li J, Huang Y, Yang J, Wang Q, et al. Bioinformatics analysis identifies TNFRSF1A as a biomarker of liver injury in sepsis TNFRSF1A is a biomarker for septic liver injury. Genet Res. 2022;2022:1493744.
27. Gu C, Qiao W, Wang L, Li M, Song K. Identification of genes and pathways associated with multiple organ dysfunction syndrome by microarray analysis. Mol Med Rep. 2018;18:31–40.

28. Sendler M, Weiss F-U, Golchert J, Homuth G, van den Brandt C, Mahajan UM, et al. Cathepsin B-mediated activation of trypsinogen in endocytosing macrophages increases severity of pancreatitis in mice. Gastroenterology. 2018;154:704-718.e10.
29. Zhou X-Y, Luo Y, Zhu Y-M, Liu Z-H, Kent TA, Rong J-G, et al. Inhibition of autophagy blocks cathepsins–tBid–mitochondrial apoptotic signaling pathway via stabilization of lysosomal membrane in ischemic astrocytes. Cell Death Dis. 2017;8:e2618–e2618.
30. Song X-B, Liu G, Liu F, Yan Z-G, Wang Z-Y, Liu Z-P, et al. Autophagy blockade and lysosomal membrane permeabilization contribute to lead-induced nephrotoxicity in primary rat proximal tubular cells. Cell Death Dis. 2017;8:e2863–e2863.
31. Wu M, Zhang M, Zhang Y, Li Z, Li X, Liu Z, et al. Relationship between lysosomal dyshomeostasis and progression of diabetic kidney disease. Cell Death Dis. 2021;12:958.
32. Montaser M, Lalmanach G, Mach L. CA-074, but not its methyl ester CA-074Me, is a selective inhibitor of Cathepsin B within living cells. Biol Chem. 2002. https://doi.org/10.1515/BC.2002.147/html.
33. Platnich JM, Muruve DA. NOD-like receptors and inflammasomes: a review of their canonical and non-canonical signaling pathways. Arch Biochem Biophys. 2019;670:4–14.
34. Wicherska-Pawłowska K, Wróbel T, Rybka J. Toll-like receptors (TLRs), NOD-like receptors (NLRs), and RIG-I-like receptors (RLRs) in innate immunity: TLRs, NLRs, and RLRs ligands as immunotherapeutic agents for hematopoietic diseases. Int J Mol Sci. 2021;22:13397.
35. Nakao S, Zandi S, Sun D, Hafezi-Moghadam A. Cathepsin B-mediated CD18 shedding regulates leukocyte recruitment from angiogenic vessels. FASEB J Off Publ Fed Am Soc Exp Biol. 2018;32:143–54.
36. Liu M, Lu J, Hu J, Chen Y, Deng X, Wang J, et al. Sodium sulfite triggered hepatic apoptosis, necroptosis, and pyroptosis by inducing mitochondrial damage in mice and AML-12 cells. J Hazard Mater. 2024;467: 133719.
37. Chen Y, Long T, Chen J, Wei H, Meng J, Kang M, et al. WTAP participates in neuronal damage by protein translation of NLRP3 in an m6A-YTHDF1-dependent manner after traumatic brain injury. Int J Surg Lond Engl. 2024;110:5396–408.
38. Wan H, Ban X, He Y, Yang Y, Hu X, Shang L, et al. Voltage-dependent anion channel 1 oligomerization regulates PANoptosis in retinal ischemia-reperfusion injury. Neural Regen Res. 2025. https://doi.org/10.4103/NRR.NRR-D-24-00674.

Publisher's Note